Asian Journal of Chemistry; Vol. 29, No. 9 (2017), 2065-2068

ASIAN JOURNAL OF CHEMISTRY

https://doi.org/10.14233/ajchem.2017.20828

Contribution of Edge Structure Towards Enhanced Thermal Stability of Graphene-Based Materials

GOPAL AVASHTHI, SHRIKANT S. MAKTEDAR and MAN SINGH*

School of Chemical Sciences, Central University of Gujarat, Gandhinagar-382 030, India

*Corresponding author: Fax: +91 79 23260076; Tel: +91 79 23260210; E-mail: mansingh50@hotmail.com

Received: 16 April 2017; *Accepted*: 30 May 2017; *Published online*: 15 July 2017; AJC-18492

An advanced approach for direct covalent functionalization (DCF) of graphene-based material has been developed. The functionalized graphene oxide (f-GO) has been prepared with the robust sonochemical approach with complete deletion of hazardous acylating and coupling reagents. The as-prepared f-GO was extensively characterized with various analytical techniques like near edge X-ray absorption fine structure (NEXAFS), ^{13}C SSNMR, HRXPS, HRTEM, XRD, Raman, AFM, TGA, DSC and FTIR. An investigation of thermal applications of graphene-based materials has been confined due to the conventional thermal instability of graphene oxide (GO). However, DCF through contribution of C_K edges of graphene oxide, have confirmed the significance of f-GO towards enhanced thermal stability. The total percentage weight loss in TG-DTA has confirmed an enhanced thermal stability of f-GO. The contribution of edge structure towards enhanced thermal stability has confirmed with near edge XAFS spectroscopy. The participation of various atomic domains has synergistically contributed towards enhanced thermal stability of f-GO.

Keywords: Covalent functionalization, Synergistic impact, Thermal stability, Near edge X-ray absorption fine structure spectroscopy.

INTRODUCTION

One of the natural carbon allotropes *i.e.* graphite and its oxidative product graphite oxide play an important role in the synthesis of grapheme [1-5]. The one atom thick, honeycomb-like, hexagonal 2-D graphene is most intensively studied material of 20th century for its excellent properties [6-9]. Since Andre Geim and *Konstantin Novoselov* got Nobel Prize in 2010 for the discovery and electronic study of graphene in 2004 [1-6]. The 2-D carbon-based composite materials is essentially known for various applications rather it is more promising than 1-D and 0-D nanostructured materials [6-10]. The cost-effective, conventional and greener approach is the demand of the science to maintain the sustainability of the environment to developing the new materials for various applications rather than the highly expensive physical route. Therefore, the microwave, ultrasound and conventional route are favourable for current scenario of graphene research [11-19]. The ultrasound assisted mechanical energy simultaneous rise the temperature 5000 K and instantly cooling, play a major role in the exfoliation of the graphite oxide into graphene oxide and direct covalent functionalization (DCF) through cavitation phenomenon [12-14]. Moreover, the conventional approach based direct isolation of single-layer graphene from the graphite is a challenge for the scientific community. Hence, the reduced graphene oxide (RGO) and edge-functionalized graphene oxide (f-GO) not only broaden its functionalities but also induce the electronic structure of the RGO and f-GO [20-22]. However, by using several hazardous chemicals and non-greener methods are reported for the functionalization. But the ultrasound assisted DCF of graphene oxide skips the use of the hazardous chemicals and explored for the various qualitative applications [10-14]. The f-GO has been suitable for thermally stable nanocomposite, fuel-cells, electrocatalyst, photocatalyst, supercapacitor performance and biomedical applications [23-32]. Furthermore, synthesize f-GO analyzed by various highly sophisticated analytical techniques to explore its structural confirmation [12-33]. Therefore, the thermal stability of f-GO is confirmed by TGA due to the synergistic impact of the electronic cloud towards edges of GO [13]. The edge structure of f-GO is confirmed by the high-resolution UHV X-ray photoelectron spectroscopy, Omicron ESCA+ [13,23,33].

EXPERIMENTAL

Graphite flakes, 1,3-benzoxazol-2-amine (BOZA) and 2-(1*H*-Indol-3-yl)ethanamine (2-IEA), were purchased from Sigma-Aldrich Co. Concentrated sulphuric acid (95-98 %), phosphoric acid (> 85 wt. % in H_2O), concentrated hydrogen chloride (35.4 %) and 30 % hydrogen peroxide were procured

from S.D Fine chemicals. Potassium permanganate was supplied by Rankem. Absolute alcohol was obtained from Scvuksmandli Ltd. India. All chemical are analytical grade and were used without further purification. The method employed to firstly synthesis of graphite oxide by previously reported method followed by exfoliation and ultrasound assisted direct covalent functionalization of graphene oxide [13,33].

General procedure: The as prepared graphite oxide 1 mg/mL concentration was exfoliated in ethanol [13]. The ultrasound assisted cavitation raise the temperature 5000 K, which plays important role to break the van der Waals force between the sheets of graphite oxide and single layer graphene oxide were separated out. Initially, 40 mg graphite oxide in 40 mL EtOH was exposed for the ultrasonic treatment for period of 3 h to exfoliate the single layer of graphene oxide followed by addition of 200 mg of 1,3-benzoxazol-2-amine (BOZA) and 2-(1*H*-Indol-3-yl)ethanamine (2-IEA), respectively and reaction exposed for the 20 min to each for synthesizing the edge-functionalized product. The acid catalyzed *in situ* esterification mechanism supports the formation of ester intermediate leads to amidation through nucleophilic substitution reaction. The edge-functionalized product f-(BOZA) GO and f-(2-IEA) GO was further washed with the EtOH for three times at 6000 rpm for 15 min of each to remove the unreactive impurity.

Detection method: The edge functionalization was confirmed with the high resolution UHV X-ray photoelectron spectroscopy, Omicron ESCA+ at pass energy 20 mA. The Al K_α radiations of 1486.7 eV was operated at 15 kV and 20 mA, throughout the measurements. The impact of edge structure on thermal stabilization of f-GO measured with EXSTAR TG/DTA 7300 analyser under N_2 ambient.

RESULTS AND DISCUSSION

XPS survey spectrum for edge structure determination: The compositional structure of GO, f-(BOZA) GO and f-(2-IEA) GO were analyzed with XPS spectrum in the range of 100-1000 eV (Figs. 1-3). The XPS survey spectrum of GO exposes only two peaks confirms the presence of the carbon and oxygen (Fig. 1). Moreover, the more counts of oxygen as compared to carbon in GO peaks shows the good degree of oxidation of graphite (Fig. 1a). The high-resolution C1 spectrum of GO specifies four peaks at various binding energies. These four peaks observed for four different carbon-based functionality over the surface of graphene at 283.2 (C=C), 284.3 (C-O-C), 286.4 (C=O), 288.1 eV (O-C=O) (Fig. 1b). The % compositional concentration (% CC) of carbon-based functionality calculated by Casa XPS software and these are 11.08, 30.11, 50.03 and 8.78, respectively. The oxygen-rich carbon functionality (ORCF) over the surface of graphene creates the rich electronic cloud. Thus, as the presence of ORCF over the surface of graphene, enhanced the effective nuclear force of attraction reinforced to the higher value of the electron affinity. Therefore, the ORCF over the surface of graphene is responsible for the enhancing the binding energies. Furthermore, the survey and high-resolution C1 spectrum of f-(BOZA) GO and f-(2-IEA) GO confirmed the real-time reduction and DCF of GO (Figs. 2 and 3). As compared to GO, the survey spectrum of f-(BOZA) GO and f-(2-IEA) GO analyzed with

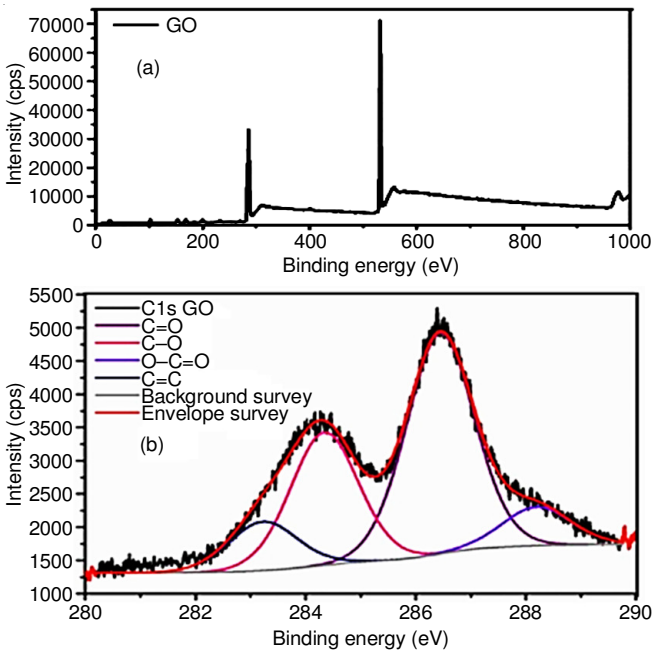

Fig. 1. XPS spectrum of GO (a), High resolution C1s spectrum of GO (b)

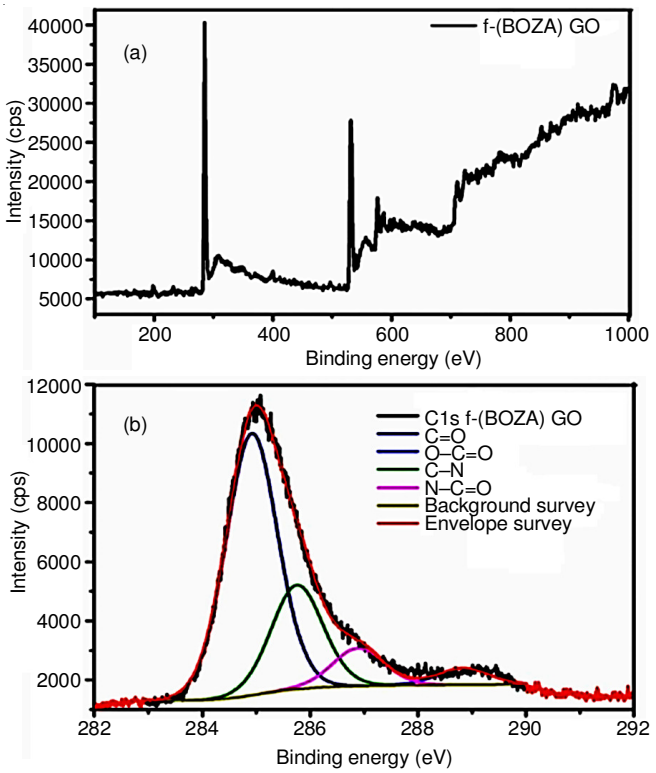

Fig. 2. XPS spectrum of f-(BOZA) GO (a), High resolution C1s spectrum of f-(BOZA) GO (b)

nitrogen based functionality over the edge of graphene along with the ORCF over the surface of graphene, respectively (Figs. 2a and 3a). The high-resolution C1 spectrum of the f-(BOZA) GO confirms the presence of C=C, -C-N-, N-C=O, O-C=O at 284.9, 285.7, 286.8, 288.8 eV, respectively (Fig. 2b). The % CC functionality calculated by Casa XPS software found as 62.33, 24.73, 8.97 and 3.98, respectively. The % CC of carbon enhances from 11.08 to 62.33 and the % CC of O-C=O decreases from

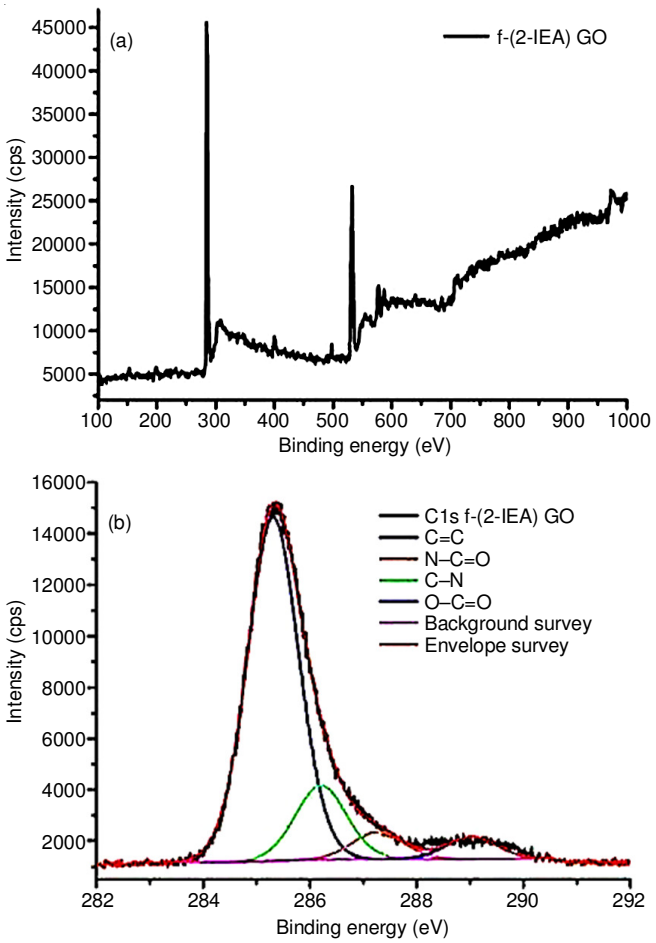

Fig. 3. XPS spectrum of f-(2-IEA) GO (a), High resolution C1s spectrum of f-(2-IEA) GO (b)

8.78 to 3.98 confirms the simultaneous reduction of GO. The deconvoluted C1 peaks of f-(BOZA) GO having -C-N-, N-C=O at 285.7, 286.8 eV confirms the direct covalent functionalization of GO with BOZA through nucleophilic substitution reaction to forming an amide bond. However, the high-resolution deconvoluted spectrum of f-(2-IEA) GO confirms the presence of the C=C, -C-N-, N-C=O, O-C=O at 285.3, 286.2, 287.3, 289.02 eV, respectively (Fig. 3b). The % CC functionality is 71.75, 16.68, 6.08 and 5.49, respectively. The enhance % CC of carbon from 11.08 to 71.71 and reduce % CC of O-C=O from 8.78 to 5.49 confirms the simultaneous reduction. The deconvoluted C1 peak of f-(2-IEA) GO having -C-N-, N-C=O at 286.2, 287.3 also confirms the direct covalent functionalization of the GO with 2-IEA through nucleophilic substitution reaction to forming an amide bond. As comparison analysis of the GO, f-(BOZA) GO and the f-(2-IEA) GO specifies the more reduction of GO during the functionalization with 2-IEA due to less % affinity of residue towards the edge structure modification with an amide bond than that of BOZA functionalization. The modified edge dependent structure-activity relationship (SAR) of GO shows more % affinity towards edge modification with the BOZA as compared to that of 2-IEA with an amide bond. As compare to f-(2-IEA) GO, the higher degree of edge amidation in f-(BOZA) GO is enhanced the electronic cloud around the edge's nucleus and shows the less thermal stability according to the higher affinity of electron-electron repulsion between the oxygen-rich carbon functionality (ORCF) and an electronic cloud of edge. The GO shows the least thermal stability due to the only presence of high ORCF over the surface of graphene.

TGA analysis for enhanced thermal stability: The thermal decomposition of graphite, GO, BOZA, IEA, f-(BOZA) GO and f-(2-IEA) GO was analyzed with the thermogravimetric analysis (TGA) by calculating the total % wt. loss as a function of temperature (Figs. 4 and 5). Hence, the measurement was done by using the dynamic nitrogen (industrial grade) with a rate of 100 mL/min with slow ramp rate at 10 °C/min over 50-600 °C. A comparison of TGA curves of starting material BOZA, 2-IEA, GO f-(BOZA) GO and f-(2-IEA) GO, depicted in Figs. 4 and 5, respectively. The total % wt. loss of BOZA was observed about 70.1 % at > 200 °C in single stage decomposition (Fig. 4). The GO also shows the single stage decomposition of total % wt. loss about 82 % at 195 °C due to decomposition of thermally labile oxygen rich carbon functionality over the surface of graphene (Figs. 4 and 5). The single stage decomposition of the BOZA and GO confirms the single crystalline behaviour of the respective compounds. However, the f-(BOZA) GO analyzed the total % wt. loss about 63.9 % at > 200 °C only. That concludes the higher thermal stability of f-(BOZA) GO than GO and BOZA (Fig. 4). The 2-IEA was measured the total % wt. loss of about 75.8 % above the 200 °C, While the f-(2-IEA) GO shows total % wt. loss about 23.3 % only above the 200 °C confirms the higher thermal stability of f-(2-IEA) GO (Fig. 5). The reduced the total % Wt. loss of f-(BOZA) GO and f-(2-IEA) GO with enhanced residues at the edge confirms it improve thermal stability. A comparative representation of thermal stability in decreasing order is:

f-(2-IEA) GO > f-(BOZA) GO > BOZA > 2-IEA > GO

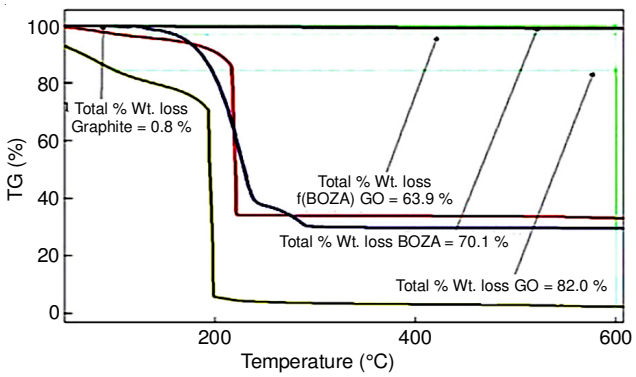

Fig. 4. Comparative TGA plot demonstrates structural stability of f-(BOZA) GO

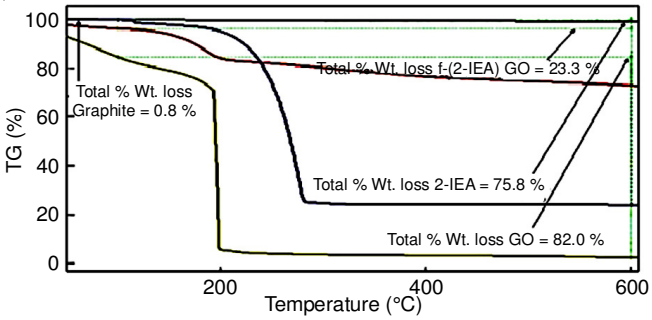

Fig. 5. Comparative TGA plot demonstrates structural stability of f-(2-IEA) GO

Conclusion

The ultrasound assisted synthesis of f-(BOZA) GO and f-(2-IEA) GO is benign and greener route to avoid the hazardous coupling reagents. However, the XPS survey spectrum confirmed the edge structure modification of functionalized graphene and presence of various functional groups over the surface of graphene. The metal-free synthesis of functionalized graphene oxide is cost-effective and demands of the current scenario of science to developing for the multifunctionality. The contribution of edge structural towards enhances thermal stability analyzed by TGA curves. In order to achieve enhance thermally stable composite materials; the graphene oxide was functionalized with the various amine substituted organic compounds for the development of metal-free thermally stable nanocomposite.

ACKNOWLEDGEMENTS

The authors are thankful to Central University of Gujarat, India and UGC for providing infrastructural and financial support.

REFERENCES

1. G. Ruess, *Monatsh. Chem.*, **76**, 381 (1947); https://doi.org/10.1007/BF00898987.
2. A. Clause, R. Plass, H.-P. Boehm and U. Hofmann, *Anorg. Allg. Chem*, **291**, 205 (1957); https://doi.org/10.1002/zaac.19572910502.
3. W. Scholz and H.P. Boehm, *Anorg. Allg. Chem.*, **369**, 327 (1969); https://doi.org/10.1002/zaac.19693690322.
4. T. Nakajima, A. Mabuchi and R. Hagiwara, *Carbon*, **26**, 357 (1988); https://doi.org/10.1016/0008-6223(88)90227-8.
5. K.S. Novoselov, A.K. Geim, S.V. Morozov, D.Z. Jiang, S.V. Dubonos, I.V. Grigorieva and A.A. Firsov, *Science*, **306**, 666 (2004); https://doi.org/10.1126/science.1102896.
6. A.K. Geim and K.S. Novoselov, *Nat. Mater.*, **6**, 183 (2007); https://doi.org/10.1038/nmat1849.
7. C. Lee, X. Wei, J.W. Kysar and J. Hone, *Science*, **321**, 385 (2008); https://doi.org/10.1126/science.1157996.
8. A.A. Balandin, S. Ghosh, W. Bao, I. Calizo, D. Teweldebrhan, F. Miao and C.N. Lau, *Nano Lett.*, **8**, 902 (2008); https://doi.org/10.1021/nl0731872.
9. M.D. Stoller, S. Park, Y. Zhu, J. An and R.S. Ruoff, *Nano Lett.*, **8**, 3498 (2008); https://doi.org/10.1021/nl802558y.
10. H.W. Kroto, J.R. Heath, S.C. O'Brien, R.F. Curl and R.E. Smalley, *Nature*, **318**, 162 (1985); https://doi.org/10.1038/318162a0.
11. S.P. Economopoulos, G. Rotas, N. Tagmatarchis, H. Shinohara and Y. Miyata, *ACS Nano*, **4**, 7499 (2010); https://doi.org/10.1021/nn101735e.
12. B. Shen, W. Zhai, D. Lu, J. Wang and W. Zheng, *RSC Adv.*, **2**, 4713 (2012); https://doi.org/10.1039/c2ra01098d.
13. S.S. Maktedar, S.S. Mehetre, M. Singh and R.K. Kale, *Ultrason. Sonochem.*, **21**, 1407 (2014); https://doi.org/10.1016/j.ultsonch.2014.02.022.
14. H. Xu and K.S. Suslick, *J. Am. Chem. Soc.*, **133**, 9148 (2011); https://doi.org/10.1021/ja200883z.
15. V. Georgakilas, M. Otyepka, A.B. Bourlinos, V. Chandra, N. Kim, K.C. Kemp, P. Hobza, R. Zboril and K.S. Kim, *Chem. Rev.*, **112**, 6156 (2012); https://doi.org/10.1021/cr3000412.
16. A. Hirsch, J.M. Englert and F. Hauke, *Acc. Chem. Res.*, **46**, 87 (2013); https://doi.org/10.1021/ar300116q.
17. D.W. Boukhvalov and M.I. Katsnelson, *Nano Lett.*, **8**, 4373 (2008); https://doi.org/10.1021/nl802234n.
18. J.X. Zhao, H.X. Wang, B. Gao, X.G. Wang, Q.H. Cai and X.Z. Wang, *J. Mol. Model.*, **18**, 2861 (2012); https://doi.org/10.1007/s00894-011-1309-8.
19. E.U. Choi, T.H. Han, J. Hong, J.E. Kim, S.H. Lee, H.W. Kim and S.O. Kim, *J. Mater. Chem.*, **20**, 1907 (2010); https://doi.org/10.1039/b919074k.
20. S. Stankovich, D.A. Dikin, R.D. Piner, K.A. Kohlhaas, A. Kleinhammes, Y. Jia, Y. Wu, S.T. Nguyen and R.S. Ruoff, *Carbon*, **45**, 1558 (2007); https://doi.org/10.1016/j.carbon.2007.02.034.
21. D. Li, M.B. Müller, S. Gilje, R.B. Kaner and G.G. Wallace, *Nat. Nanotechnol.*, **3**, 101 (2008); https://doi.org/10.1038/nnano.2007.451.
22. V.C. Tung, M.J. Allen, Y. Yang and R.B. Kaner, *Nat. Nanotechnol.*, **4**, 25 (2009); https://doi.org/10.1038/nnano.2008.329.
23. S.S. Mehetre, S.S. Maktedar, M. Singh and R.K. Kale, *Appl. Surf. Sci.*, **366**, 514 (2016); https://doi.org/10.1016/j.apsusc.2016.01.108.
24. S.S. Maktedar, S.S. Mehetre, G. Avashthi, M. Singh, T. Jayaraman and M. Jagannatha, In Proceedings of International Conference on Recent Advances in Material and Chemical Sciences (ICRAMCS), Bundelkhand University, Jhansi, India, pp 1-4 (2016).
25. M. Mamlouk, S.M.S. Kumar, P. Gouerec and K. Scott, *J. Power Sources*, **196**, 7594 (2011); https://doi.org/10.1016/j.jpowsour.2011.04.045.
26. N.A. Anastasijevic, V.B. Vesovic and R.R. Adzic, *J. Electroanal. Chem.*, **229**, 305 (1987); https://doi.org/10.1016/0022-0728(87)85148-3.
27. K. Krishnamoorthy, R. Mohan and S.J. Kim, *Appl. Phys. Lett.*, **98**, 244101 (2011); https://doi.org/10.1063/1.3599453.
28. B. Zhao, P. Liu, Y. Jiang, D. Pan, H. Tao, J. Song, T. Fang and W. Xu, *J. Power Sources*, **198**, 423 (2012); https://doi.org/10.1016/j.jpowsour.2011.09.074.
29. Z. Liu, J.T. Robinson, X. Sun and H. Dai, *J. Am. Chem. Soc.*, **130**, 10876 (2008); https://doi.org/10.1021/ja803688x.
30. O. Akhavan and E. Ghaderi, *ACS Nano*, **4**, 5731 (2010); https://doi.org/10.1021/nn101390x.
31. X. Sun, Z. Liu, K. Welsher, J. Robinson, A. Goodwin, S. Zaric and H. Dai, *Nano Res.*, **1**, 203 (2008); https://doi.org/10.1007/s12274-008-8021-8.
32. H. Chen, M.B. Müller, K.J. Gilmore, G.G. Wallace and D. Li, *Adv. Mater.*, **20**, 3557 (2008); https://doi.org/10.1002/adma.200800757.
33. D.C. Marcano, D.V. Kosynkin, J.M. Berlin, A. Sinitskii, Z. Sun, A. Slesarev, L.B. Alemany, W. Lu and J.M. Tour, *ACS Nano*, **4**, 4806 (2010); https://doi.org/10.1021/nn1006368.